The Plant Cell, Vol. 18, 2341–2355, September 2006, www.plantcell.org © 2006 American Society of Plant Biologists

# Mitochondria-Associated Hexokinases Play a Role in the Control of Programmed Cell Death in *Nicotiana benthamiana* [W]

**Moonil Kim,[a,1] Jeong-Hwa Lim,[b,1,2] Chang Sook Ahn,[c] Kyoungsook Park,[a] Gyung Tae Kim,[d] Woo Taek Kim,[c] and Hyun-Sook Pai[c,3]**

[a] BioNanotechnology Research Center, Korea Research Institute of Bioscience and Biotechnology, Taejon 305-333, Korea
[b] Division of Bioscience and Bioinformatics, Myongji University, Yongin, Kyonggi-do 449-728, Korea
[c] Department of Biology, Yonsei University, Seoul 120-749, Korea
[d] Faculty of Plant Biotechnology, Dong-A University, Pusan 604-714, Korea

**Recent findings suggest a pivotal role for mitochondria-associated hexokinase in the regulation of apoptosis in animal cells. In this study, virus-induced gene silencing (VIGS) of a hexokinase-encoding *Hxk1* caused necrotic lesions on leaves, abnormal leaf morphology, and retarded plant growth in *Nicotiana benthamiana*. Hxk1 was associated with the mitochondria, and this association required the N-terminal membrane anchor. VIGS of *Hxk1* reduced the cellular glucose-phosphorylating activity to ~31% of control levels without changing the fructose-phosphorylating activity and did not alter hexose phosphate content severely. The affected cells showed programmed cell death (PCD) morphological markers, including nuclear condensation and DNA fragmentation. Similar to animal cell apoptosis, cytochrome *c* was released into the cytosol and caspase-9– and caspase-3–like proteolytic activities were strongly induced. Furthermore, based on flow cytometry, *Arabidopsis thaliana* plants overexpressing *Arabidopsis* HXK1 and HXK2, both of which are predominantly associated with mitochondria, exhibited enhanced resistance to $H_2O_2$- and α-picolinic acid–induced PCD. Finally, the addition of recombinant Hxk1 to mitochondria-enriched fractions prevented $H_2O_2$/clotrimazole-induced cytochrome *c* release and loss of mitochondrial membrane potential. Together, these results show that hexokinase critically regulates the execution of PCD in plant cells, suggesting a link between glucose metabolism and apoptosis.**

## INTRODUCTION

Sugars serve fundamental roles as metabolic nutrients and structural components for most organisms. In plants, sugars regulate many vital developmental and metabolic processes, including germination, plant growth, photosynthesis, carbon and nitrogen metabolism, flowering, stress responses, and senescence (Rolland and Sheen, 2005). However, the mechanisms of signal transduction through sugars and the integration of sugar signals to modulate plant growth and development are still largely unknown.

In bacteria, yeast, animals, and plants, hexokinases not only catalyze sugar phosphorylation as the first step of hexose metabolism but also sense glucose levels and transmit the sugar signal to the nucleus (Stulke and Hillen, 1999; Rolland et al., 2001; Rolland and Sheen, 2005). Consistent with a role of plant hexokinases in sugar signaling, transgenic *Arabidopsis thaliana* plants overexpressing sense or antisense hexokinase genes exhibited altered sugar responses in seedling development and gene expression (Jang et al., 1997). Analyses of an *Arabidopsis HXK1* mutant (*gin2*) demonstrated that glucose signaling could be uncoupled from glucose metabolism, because *HXK1* mutants lacking catalytic activity still supported various signaling functions in gene expression, plant growth, and leaf expansion and senescence (Moore et al., 2003). Furthermore, characterization of glucose-insensitive and glucose-oversensitive mutants revealed extensive connections between glucose and plant hormone signaling pathways, including the ethylene, abscisic acid, and auxin/cytokinin pathways (Leon and Sheen, 2003; Moore et al., 2003).

Multiple isoforms of hexokinases are found in most organisms. Mammalian genomes encode a low-affinity glucokinase and three high-affinity hexokinases (I, II, and III) (Wilson, 2003). *Arabidopsis* has six hexokinase genes. The isoforms of hexokinases interact not only with each other to form dimers but also with other proteins and with various cellular membranes (Frommer et al., 2003). Hexokinase isoforms have been found in the cytosol as well as associated with the endoplasmic reticulum and plasma membrane (Travis et al., 1999). Hexokinases have also been localized to mitochondria, the chloroplast outer envelope, chloroplast stroma, and the nucleus (Galina et al., 1995; Wiese et al., 1999; Yanagisawa et al., 2003; Giese et al., 2005). This diversity of subcellular localizations of hexokinases may reflect their roles in a variety of cellular processes.

Recent evidence indicates that the mitochondria-associated hexokinase plays an important role in the control of apoptosis in mammals (Downward, 2003; Birnbaum, 2004; Majewski et al.,

[1] These authors contributed equally to this work.
[2] Current address: Biohelix, 32 Tozer Road, Beverly, MA 01915.
[3] To whom correspondence should be addressed. E-mail hspai@yonsei.ac.kr; fax 82-2-312-5657.
The author responsible for distribution of materials integral to the findings presented in this article in accordance with the policy described in the Instructions for Authors (www.plantcell.org) is: Hyun-Sook Pai (hspai@yonsei.ac.kr).
[W] Online version contains Web-only data.
www.plantcell.org/cgi/doi/10.1105/tpc.106.041509

2004). The mitochondrial pathway of apoptosis is initiated through the release of mitochondrial cytochrome *c* into the cytosol through the permeability transition (PT) pore in response to cellular stresses. Cytochrome *c* release is a major checkpoint in the initiation of apoptosis and induces the assembly of the caspase-9–activating complex, the apoptosome, in the cytosol. Within the apoptosome, caspase-9 is activated and propagates a cascade of additional caspase activation events. Hexokinase is an integral component of the PT pore through its interaction with porin or the voltage-dependent anion channel (VDAC) (Wilson, 2003), and hexokinase binding to the VDAC interferes with the opening of the PT pore, thereby inhibiting cytochrome *c* release and apoptosis (Pastorino et al., 2002; Azoulay-Zohar et al., 2004). Thus, detachment of hexokinase from the mitochondria potentiated, and its overexpression inhibited, mitochondrial dysfunction and cell death induced by various stimuli (Gottlob et al., 2001; Bryson et al., 2002; Majewski et al., 2004). Recent studies have shown that cyclophilin D, another component of the PT pore, is a key factor in the regulation of PT pore function and that cyclophilin D–dependent mitochondrial PTs are required to mediate some forms of necrotic cell death but not apoptotic cell death (Baines et al., 2005; Nakagawa et al., 2005). However, these observations do not exclude the possibility that certain forms of apoptosis are mediated by the mitochondrial PT, because some forms of apoptosis are significantly inhibited by cyclosporin A, a specific inhibitor of cyclophilin activity (Green and Kroemer, 2004). Additionally, cyclophilin D–overexpressing mice exhibited an increase in apoptotic heart muscle cells (Baines et al., 2005). Furthermore, in cancer cells, cyclophilin D overexpression suppresses apoptosis via the stabilization of hexokinase II binding to the mitochondria (Machida et al., 2006).

In this study, we used tobacco rattle virus (TRV)–based virus-induced gene silencing (VIGS) to assess the functions of various signaling genes in *Nicotiana benthamiana*. This functional genomic screen revealed that VIGS of a hexokinase gene, *Hxk1*, induced the spontaneous formation of necrotic lesions in leaves. Hxk1 was associated with the mitochondria, and its expression was stimulated by various cell death–inducing stresses. VIGS of *Hxk1* resulted in apoptotic cell death in leaves, indicating that depletion of mitochondrial hexokinases activated programmed cell death (PCD). Conversely, overexpression of the mitochondria-associated *Arabidopsis* hexokinases, HXK1 and HXK2, conferred enhanced resistance to oxidative stress–induced cell death. Finally, the exogenous addition of recombinant Hxk1, but not Hxk1ΔN, which lacks the membrane anchor, inhibited clotrimazole (CTZ)/$H_2O_2$–induced cytochrome *c* release from mitochondria. These results suggest a direct link between plant hexokinases and the PCD process.

## RESULTS

### Isolation of *Hxk1* and Comparison with Plant Hexokinases

For functional genomics using VIGS, ~15,000 ESTs were sequenced from three cDNA libraries constructed from various tissues of *N. benthamiana*, and selected cDNAs, mostly encoding a signaling gene, were subjected to VIGS. The partial *Hxk1* cDNA used in the initial VIGS screening was ~0.9 kb in length. To obtain the full-length cDNA of *Hxk1*, 5′-rapid amplification of cDNA ends PCR was performed using RNA isolated from *N. benthamiana* seedlings. The full-length *Hxk1* cDNA encodes a polypeptide of 497 amino acids with a predicted molecular mass of 53,889.94 D (see Supplemental Figure 1 online). The predicted Hxk1 protein has an N-terminal membrane-anchoring sequence, a hexokinase signature, a phosphate binding motif, a sugar recognition motif, and an ATP binding motif (see Supplemental Figure 1 online). Based on the amino acid sequence, Hxk1 falls into the group of plant hexokinases with an N-terminal hydrophobic membrane anchor, including HXK1 and HXK2 from *Arabidopsis*, Hxk2 from *Solanum lycopersicum*, HK1 and HK2 from *Solanum tuberosum*, and HxK1 from *Spinacia oleracea* (see Supplemental Figure 1 online). Among the six hexokinase genes in *Arabidopsis*, *Hxk1* is closely related to HXK1 and HXK2 but not to the other hexokinase genes (data not shown).

### The Hxk1 Membrane Anchor Is Required for Mitochondrial Localization

We examined the subcellular localization of Hxk1 by expressing Hxk1:GFP, in which the full-length Hxk1 (Met-1 to Ser-497) was fused to the green fluorescent protein (GFP). The DNA construct encoding Hxk1:GFP under the control of the cauliflower mosaic virus 35S promoter was introduced into protoplasts isolated from *Arabidopsis* seedlings (Figure 1). To track mitochondria, a construct encoding an $F_1$ATPase-γ:RFP fusion protein of the mitochondrial $F_1$ATPase γ-subunit and red fluorescent protein (RFP) was cotransformed into the protoplasts. After incubation at 25°C for 24 h, gene expression was examined by confocal laser scanning microscopy to capture GFP, RFP, and chlorophyll autofluorescence images. Most of the Hxk1:GFP signal overlapped with the $F_1$ATPase-γ:RFP signal, demonstrating that the fusion protein is targeted primarily to the mitochondria (Figure 1).

To examine whether the N-terminal sequence encoding the membrane anchor plays a role in the mitochondrial targeting of Hxk1, we examined the localization of Hxk1ΔN (Met-28 to Ser-497), the N-terminal deletion form of Hxk1 (Figure 1). Following the membrane anchor sequence, the N terminus of Hxk1 contains another in-frame translation initiation codon (Met-28) (indicated by the arrow in Supplemental Figure 1 online), which is conserved in most plant hexokinases that have the anchor sequence. The GFP signal of Hxk1ΔN:GFP no longer overlapped with the RFP signal, indicating that the protein was no longer associated with the mitochondria. Instead, its GFP signal was distributed throughout the cytosol, as it was in the GFP control (Figure 1). These results demonstrate that the N-terminal membrane anchor sequence is required for the mitochondrial association of Hxk1.

### Expression of *Hxk1*

The expression pattern of the *Hxk1* gene was investigated using semiquantitative RT-PCR and RNA gel blot analysis (see Supplemental Figure 2 online). Using semiquantitative RT-PCR, the *Hxk1* mRNA was detected in all tissues of *N. benthamiana* examined (see Supplemental Figure 2A online). The mRNA was relatively abundant in open flowers, flower buds, and young

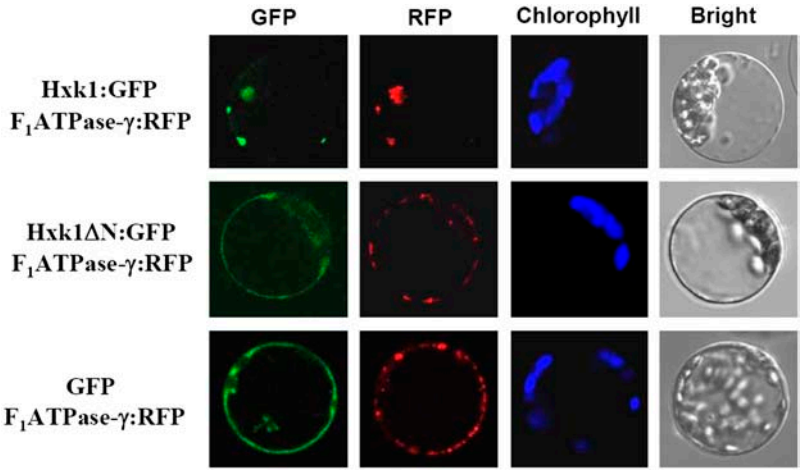


**Figure 1.** Association of Hxk1 with Mitochondria.

The subcellular localization of the GFP fusion proteins of the full-length Hxk1 (Met-1 to Ser-497) and the N-terminal deletion mutant Hxk1ΔN (Met-28 to Ser-497), which lacks the N-terminal membrane anchor sequence, was analyzed. *Arabidopsis* protoplasts were cotransformed with Hxk1:GFP or Hxk1ΔN:GFP and the $F_1$ATPase-γ:RFP construct, and the localization of fluorescent signals was examined at 24 h after transformation by confocal laser scanning microscopy. Chloroplasts and mitochondria were visualized by chlorophyll autofluorescence and red fluorescence of the $F_1$ATPase-γ:RFP, respectively. GFP, RFP, chlorophyll autofluorescence, and bright-field images are shown.

leaves but was detected at lower levels in mature leaves, stems, and roots of *N. benthamiana* (see Supplemental Figure 2A online). The *Hxk1* mRNA levels in the leaves increased 6 h after $H_2O_2$ or heat (55°C) treatment (see Supplemental Figure 2B online), both of which activate PCD in plant cells (Desikan et al., 1998; Balk et al., 1999; Houot et al., 2001). Furthermore, the *Hxk1* mRNA level in leaves increased in response to thapsigargin, particularly when the leaves were pretreated with cycloheximide (see Supplemental Figure 2C online). Thapsigargin irreversibly inhibits the $Ca^{2+}$-ATPase of the endoplasmic reticulum and increases cytosolic $Ca^{2+}$ levels to induce apoptosis in animals and causes endoplasmic reticulum stress in plants (Lilliehook et al., 2002; Ordenes et al., 2002). Thus, *Hxk1* expression seems to be stimulated by increased cytosolic $Ca^{2+}$ levels, particularly when protein synthesis is blocked. Together, these results indicate that *Hxk1* expression is stimulated by diverse cellular stresses that induce PCD.

### VIGS Phenotypes and Suppression of the *Hxk1* Transcripts in the VIGS Lines

To induce gene silencing of *Hxk1*, we cloned three different cDNA fragments of *Hxk1* into the TRV-based VIGS vector pTV00 (Ratcliff et al., 2001) and infiltrated *N. benthamiana* plants with *Agrobacterium tumefaciens* containing each plasmid (Figure 2A). TRV:D1 and TRV:D2 contain 0.72-kb N-terminal and 0.76-kb C-terminal regions of the *Hxk1* cDNA, respectively, whereas TRV:F contains the full-length cDNA. VIGS with each of these constructs resulted in the formation of necrotic lesions on leaves, abnormal leaf development, and reduced plant height (Figure 2B). The lesions containing brownish cells began as a small spot or stripe of collapsed tissue, usually appearing in the middle to lower part of the young leaves at ~10 d after infiltration. Interestingly, the lesions were found only in leaves. In Evans blue–stained leaves, single cells or cell groups corresponding to sites of the lesions were intensely stained (Figure 2B, brown arrows), suggesting localized cell death. The cell death sometimes progressed to the complete collapse and disappearance of the leaf tissues. Abnormal leaf morphology was also observed in the TRV:Hxk1 lines. Newly emerged leaves were small, narrow, and wrinkled and occasionally showed abnormal vascular patterning.

The effects of gene silencing on the endogenous level of *Hxk1* mRNA were examined using semiquantitative RT-PCR (Figure 2C) because the level of transcript in the leaves was very low. RT-PCR using the HXK-A primers (indicated in Figure 2A) produced significantly less PCR product in the TRV:D1 VIGS lines compared with the TRV control, indicating that the expression of *Hxk1* was significantly reduced in the VIGS lines. The same primers detected high levels of viral genomic transcripts containing the C-terminal region of *Hxk1* in the TRV:F and TRV:D2 lines. RT-PCR with the HXK-B primers (Figure 2A) indicated reduced amounts of PCR product in the TRV:D2 line compared with the TRV control, suggesting silencing of the endogenous *Hxk1* gene, whereas the same primers detected high levels of viral transcripts containing the N-terminal region of *Hxk1* in the TRV:F and TRV:D1 lines. No PCR product was detected by RT-PCR with the HXK-C primers (Figure 2A) in the TRV:D1 line, whereas viral genomic transcripts containing the C-terminal region of *Hxk1* were detected in the TRV:F and TRV:D2 lines. The transcript levels of actin remained constant. Together, these results demonstrate that the expression of *Hxk1* was suppressed in these VIGS lines.

### Hexokinase Activity and Hexose Phosphate Content in the VIGS Lines

To analyze whether the silencing of *Hxk1* resulted in reduced hexokinase activity, we measured glucose and fructose phosphorylation activity using protein extracts isolated from TRV and

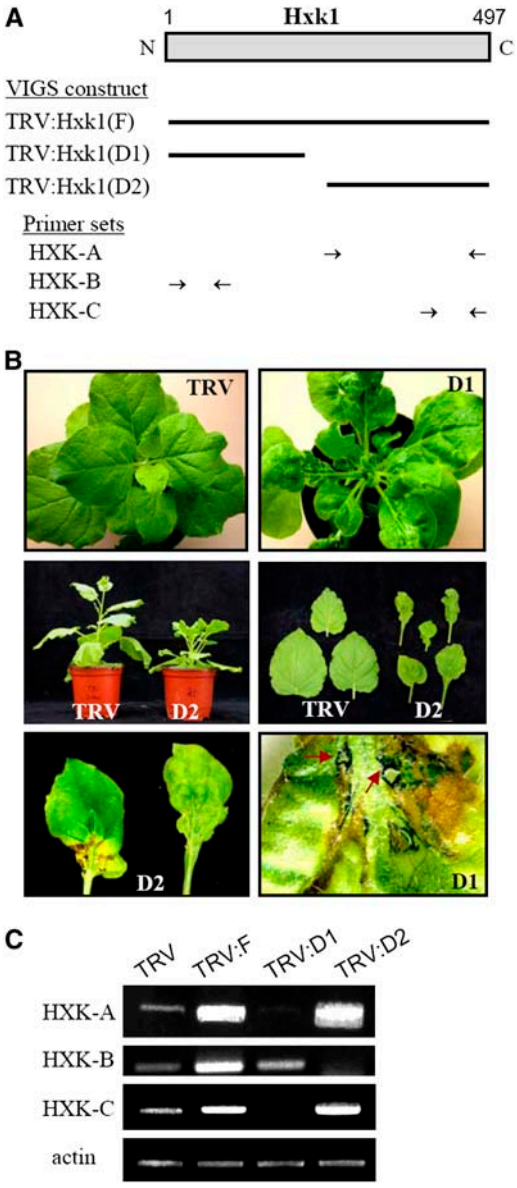


**Figure 2.** VIGS Constructs, Phenotypes, and Suppression of the *Hxk1* Transcripts.

**(A)** Scheme of the structure of Hxk1, and three VIGS constructs containing different regions of the *Hxk1* cDNA (marked by bars). *N. benthamiana* plants were infected with *Agrobacterium* containing the TRV control and three different forms of TRV:Hxk1 constructs. The positions of the primer sets, HXK-A, HXK-B, and HXK-C, used for RT-PCR analyses are indicated.

**(B)** Necrotic lesion phenotypes of the Hxk1 VIGS line. Photographs of leaves and whole plants were taken at 20 d after inoculation. The leaf tissues undergoing cell death are marked with arrows in the Evans blue–stained leaves (bottom right).

**(C)** Semiquantitative RT-PCR analysis to examine the transcript levels of *Hxk1*. RNA was extracted from the fourth leaf above the infiltrated leaves from *N. benthamiana* plants infected with TRV, TRV:Hxk1(F), TRV:Hxk1(D1), or TRV:Hxk1(D2). The HXK-A, HXK-B, and HXK-C primers were used for PCR. As a control for RNA amount, the actin mRNA level was examined.

TRV:Hxk1 VIGS lines. Leaves of the TRV:Hxk1 plants displayed ~31% of the glucose phosphorylation activity of the TRV control leaves, whereas the fructose phosphorylation activity was similar to that of the control (Figure 3A). Because hexokinases have a preferential affinity for glucose, these results suggest that VIGS of *Hxk1* reduced the hexokinase protein level in the affected cells.

The cellular glucose-6-phosphate and fructose-6-phosphate contents were also measured using leaf extracts isolated from the TRV and TRV:Hxk1 VIGS lines. In TRV:Hxk1 plants, glucose-6-phosphate content was ~76% of that of the TRV control, whereas the fructose-6-phosphate content was almost identical to that of the control, indicating that the overall hexose phosphate content was not severely altered (Figure 3B). Thus, it is unlikely that the cell death in TRV:Hxk1 plants was caused by a general deficiency of hexose phosphates.

### Phenotypes of PCD

We examined the nuclear morphology of cells in the abaxial epidermal layer from leaves of the VIGS lines by 4′,6-diamidino-2-phenylindole staining (Figure 4A). In epidermal cells of the

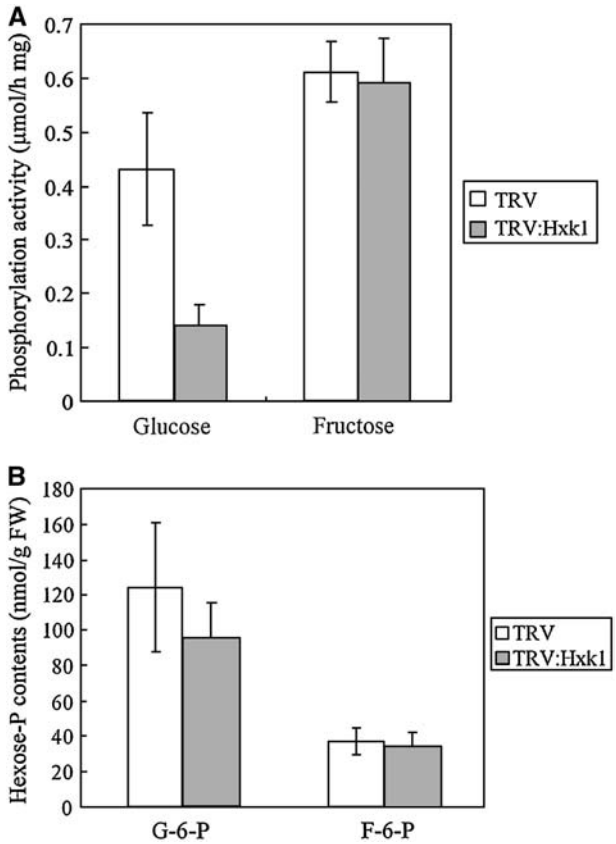


**Figure 3.** Hexokinase Activity and Hexose Phosphate Content.

Total cell extracts were prepared from the fourth leaf above the infiltrated leaves from the TRV and TRV:Hxk1 VIGS lines. Error bars represent SD. Glucose and fructose phosphorylation activity, and the amounts of glucose-6-phosphate (G-6-P) and fructose-6-phosphate (F-6-P) in the cell extracts, are shown. FW, fresh weight.

TRV:Hxk1 leaves, compaction and shrinkage of the nucleus compared with control lines was evident. The epidermal layer of the TRV:Hxk1 leaves contained elongated cells with a simplified structure (arrow), particularly in the area surrounding the necrotic lesion, whereas the control leaf epidermis contained normal pavement cells (Figure 4A). Furthermore, DNA laddering was observed in genomic DNA isolated from the TRV:Hxk1 line (Figure 4B). DNA ladders are formed during PCD as a result of the activation of cell death–specific endonucleases that cleave the nuclear DNA into oligonucleosomal units. Oligonucleosomal DNA fragmentation was observed with the total genomic DNA probe only in the Hxk1 VIGS line (Figure 4B). Because nuclear condensation and DNA laddering are the hallmark features of PCD, these results demonstrate that reduced expression of *Hxk1* activates a PCD pathway in plants.

### Localization of Cell Death in Leaf Cell Layers

Transverse leaf sections demonstrated that TRV control leaves had the typical leaf structure of dicotyledonous plants with

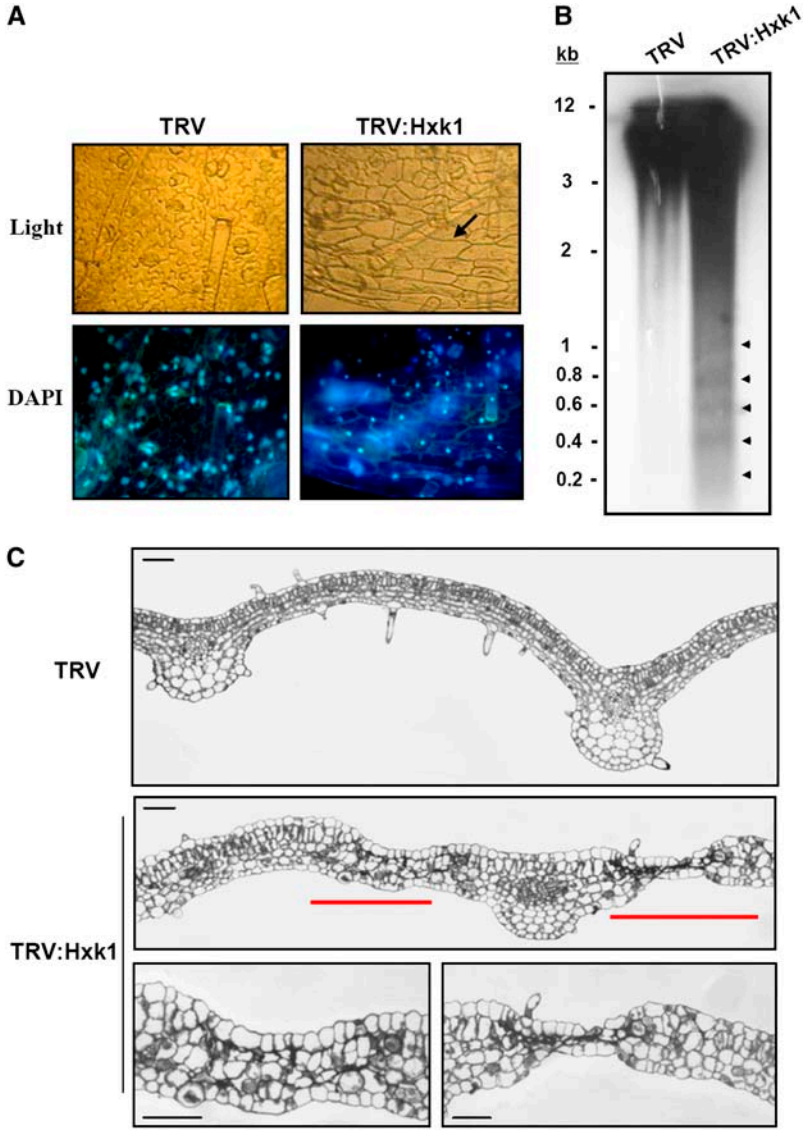


**Figure 4.** Phenotypes of PCD.

**(A)** Nuclear condensation. Light and fluorescence micrographs of abaxial leaf epidermal cells from TRV and TRV:Hxk1 VIGS lines after nuclear staining with 4′,6-diamidino-2-phenylindole (DAPI; 100 μg/mL). Elongated epidermal pavement cells in the HXK1 VIGS line are indicated by the arrow.
**(B)** Oligonucleosomal DNA fragmentation. Genomic DNA gel blot analysis was performed with DNA extracted from the leaves of the VIGS lines using the total genomic DNA of *N. benthamiana* as a probe.
**(C)** Light micrographs of leaf transverse sections. Leaf areas containing degenerating palisade and mesophyll cells are marked with red bars in TRV:Hxk1 VIGS cells. Enlarged views of the disintegrating regions are shown at bottom. Bars = 100 μm.

distinct adaxial and abaxial epidermal layers (Figure 4C). In TRV:Hxk1 plants, the lamina was thicker as a result of a moderate increase in cell size (Figure 4C). The typical dorsoventral organization of the palisade and mesophyll cells was maintained in the TRV:Hxk1 leaves for the most part, but in some areas, particularly around the necrotic lesions, spherical cells were observed and the palisade layer was not distinguishable. In TRV:Hxk1 leaves, cells in the palisade and mesophyll layers started to degenerate first, followed by complete disintegration of the leaf.

### Involvement of Reactive Oxygen Species

To investigate whether reactive oxygen species (ROS) are generated in cells undergoing PCD in the VIGS lines, we prepared protoplasts from leaves of the TRV and TRV:Hxk1 lines and incubated the protoplasts with 2′,7′-dichlorodihydrofluorescein diacetate ($H_2$DCFDA), which produces a green fluorescent signal when chemically modified by $H_2O_2$ (Figure 5A). $H_2$DCFDA is a cell-permeant indicator for ROS that is nonfluorescent until the acetate groups are removed by intracellular esterases and oxidation occurs within the cell (Bethke and Jones, 2001). The accumulation of fluorescent $H_2$DCFDA in protoplasts from the TRV:Hxk1 VIGS lines was significantly higher than that of the TRV control. The mean fluorescence for protoplasts from the TRV:Hxk1 lines was ~7.5-fold higher than that of the TRV control (Figure 5A). These results demonstrate that ROS are involved in this cell death program. TRV:Hxk1 leaves exhibited 2.5-fold higher levels of relative ion leakage than leaves from the TRV control (Figure 5B). In necrotic lesions caused by the hypersensitive response (HR), lignin deposition plays an important role in increasing the mechanical strength of cell walls and inhibiting pathogen invasion (Nimchuk et al., 2003). Leaves from the VIGS lines were stained with phloroglucinol-HCl, and an increase in lignin staining was observed in leaf cells of the TRV:Hxk1 line (Figure 5C).

### Expression of the Defense Genes

We examined whether Hxk1-mediated PCD induces the expression of defense-related genes using semiquantitative RT-PCR (Figure 5D). The *PR1a*, *PR1b*, *PR1c*, *PR2*, *PR4*, *PR5*, *S25-PR6*, *SAR8.2a*, *HSR203J*, *HIN1*, and *630* genes are all strongly induced during HR cell death (Heath, 2000). *NTCP-23* (a Cys protease) and *p69d* (a Ser protease) are involved in pathogen-induced cell death, whereas the chloroplastic *ClpP* protease plays a role in chloroplast development but not in senescence or HR cell death (Beers et al., 2000). Among these genes, *PR1a*, *PR1c*, *PR2*, *PR5*, *HSR203J*, *SAR8.2*, *HIN1*, *NTCP-23*, *p69d*, and *ClpP* genes were transcriptionally induced in the TRV:Hxk1 line. Expression of *SGT1*, *RAR1*, and *SKP1*, signaling genes in plant defense (Austin et al., 2002; Azevedo et al., 2002), as well as actin expression remained constant. Thus, hexokinase-mediated PCD promotes the expression of many of the PR genes induced during HR cell death, indicating that some features of HR cell death are conserved in the hexokinase-mediated PCD process.

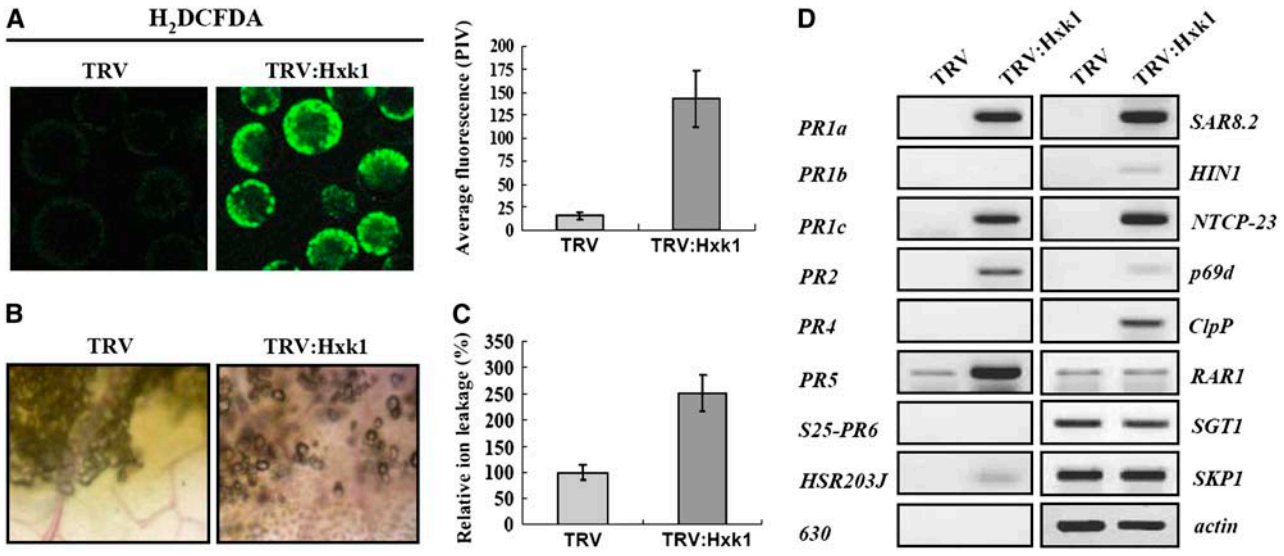


**Figure 5.** Involvement of ROS and the Accumulation of Defense Markers during Cell Death.

**(A)** ROS production. Protoplasts isolated from leaves of TRV or TRV:Hxk1 VIGS lines were incubated in 2 μM $H_2$DCFDA for 90 s. $H_2$DCFDA is a ROS indicator that becomes fluorescent when oxidized by ROS within the cell. The fluorescence of protoplasts from the TRV and TRV:Hxk1 VIGS lines was quantified by pixel intensity. Data points represent means ± SD of 13 to 16 individual protoplasts. PIV, pixel intensity value.
**(B)** Lignin deposition. Leaf samples were incubated in a phloroglucinol-HCl solution for 2 min. Lignin staining appears pink.
**(C)** Relative ion leakage. Data points are indicated as relative values (TRV = 100%). Means ± SD of three experiments per line are indicated.
**(D)** Semiquantitative RT-PCR analysis to examine transcript levels of cell death– and defense–related genes. Total RNA was extracted from the fourth leaf above the infiltrated leaves from the TRV and TRV:Hxk1 lines. As a control for RNA amounts, actin mRNA levels were examined.

### Disrupted Mitochondrial Membrane Potential and Release of Cytochrome *c*

During apoptosis in animal cells, modification of mitochondrial membrane permeability initiates the cell death pathway. The mitochondrial membrane potential of the protoplasts isolated from leaves of TRV controls and TRV:Hxk1 VIGS lines was monitored by TMRM fluorescence (Figure 6A). TMRM is a lipophilic cationic dye that accumulates in mitochondria in proportion to the mitochondrial membrane potential (Zhang et al., 2001). A decrease in the membrane potential leads to a decrease in fluorescence as a result of the diminished capacity of mitochondria to retain the probe. The average fluorescence of protoplasts from TRV:Hxk1 leaves was only 12.5% of that of the TRV control, indicating the disruption of mitochondrial membrane potential.

During apoptosis in animal cells, the release of cytochrome *c* occurs before visible morphological changes. We investigated cytochrome *c* release during PCD. Leaves of the VIGS lines were homogenized and mitochondria were separated from the cytosol by differential centrifugation. Proteins in each fraction were examined by protein gel blot analysis to detect cytochrome *c* and the mitochondrial VDAC (or porin) as a control for fractionation (Figure 6B). Cytochrome *c* was detected primarily in the mitochondria in the TRV control, whereas it was detected in the cytosolic fraction in the TRV:Hxk1 lines. VDAC, which forms a channel in the outer membrane of mitochondria (Tsujimoto and Shimizu, 2002), was detected only in the mitochondrial fraction. This result shows that cytochrome *c* is released from the mitochondria into the cytosol, similar to the early events of apoptosis in animal cells, during PCD in the Hxk1 VIGS lines.

### Activation of Caspase-Like Activity

During apoptosis in animal cells, cytosolic cytochrome *c* induces the assembly of the caspase-9–activating complex, which in turn propagates a cascade of further caspase activation, including caspase-3. Although plants lack direct homologs of caspase genes, caspase-like protease activities have been detected in HR cell death and in PCD associated with other nonpathogenic responses, such as heat, menadione, and isopentenyladenosine treatment (del Pozo and Lam, 1998; Balk et al., 1999; Sun et al., 1999; Mlejnek and Prochazka, 2002). Furthermore, caspase inhibitors markedly suppress plant cell death and the associated symptoms of apoptosis in several cases (Danon et al., 2004; Thomas and Franklin-Tong, 2004). Using synthetic fluorogenic substrates for animal caspase-9 (LEHD-AFC) and caspase-3 (DEVD-AFC), we found that the leaf protein extract from two different TRV:Hxk1 lines exhibited both caspase-9–like and caspase-3–like proteolytic activities (Figure 6C). Activation of caspase-like protease activity could not be detected in TRV control leaves.

### Enhanced Resistance of *HXK1*- and *HXK2*-Overexpressing *Arabidopsis* Plants to $H_2O_2$- and $\alpha$-Picolinic Acid–Induced Cell Death

Exogenous $H_2O_2$ induces a typical PCD in *Arabidopsis* and *N. benthamiana* cell cultures (Desikan et al., 1998; Houot et al., 2001). We tested whether hexokinase overexpression suppresses $H_2O_2$- and $\alpha$-picolinic acid–induced cell death using transgenic *Arabidopsis* plants overexpressing the *Arabidopsis* hexokinase genes *HXK1* and *HXK2* (Figure 7). *Arabidopsis* HXK1 and HXK2 have N-terminal membrane anchors and are localized primarily in mitochondria (B. Moore and J. Sheen, unpublished data, cited in Rolland and Sheen, 2005). Overexpression of these hexokinase genes resulted in altered sugar responses in seedling development and gene expression in *Arabidopsis* (Jang et al., 1997; Xiao et al., 2000). To examine the effect of $H_2O_2$, protoplasts isolated from 3-week-old wild-type and transgenic plants were treated with 10 mM $H_2O_2$ for 3, 6, 12, and 24 h to induce cell death, stained with propidium iodide, and analyzed by flow cytometry. Cells with damaged membranes allowed propidium iodide to enter the cell and fluoresce red. After $H_2O_2$ treatment, the hexokinase-overexpressing lines displayed a reduction in the numbers of dead protoplasts, compared with the wild-type lines (Figure 7A; data not shown). By 6 h after $H_2O_2$ treatment, percentages of live protoplasts were 23.35, 33.85, and 42.55% for the wild-type, *HXK1*-overexpressing, and *HXK2*-overexpressing *Arabidopsis* lines, respectively (Figure 7A). Interestingly, *HXK2* expression repeatedly conferred a higher survival rate on protoplasts than *HXK1* expression in response to $H_2O_2$.

Similarly, protoplasts isolated from the wild-type, *HXK1*-overexpressing, and *HXK2*-overexpressing *Arabidopsis* plants were treated with 0.5 mg/mL $\alpha$-picolinic acid for 3 h and analyzed by flow cytometry after propidium iodide staining. $\alpha$-Picolinic acid triggers HR-like cell death in rice (*Oryza sativa*) leaves and suspension cell cultures (Zhang et al., 2004). After $\alpha$-picolinic acid treatment, percentages of live protoplasts for the wild-type, *HXK1*-overexpressing, and *HXK2*-overexpressing *Arabidopsis* lines were 74.56, 95.29, and 97.56%, respectively, indicating that hexokinase overexpression was correlated with higher survival rates (Figure 7B). Together, these results suggest that the increased hexokinase activity partially protects cells from $H_2O_2$- and $\alpha$-picolinic acid–induced PCD.

### Exogenously Added Hxk1 Inhibits CTZ/$H_2O_2$-Induced Cytochrome *c* Release from the Mitochondria-Enriched Fraction

It has been shown in mammals that hexokinase is an integral component of the PT pore through its interaction with VDAC, and hexokinase binding to VDAC suppresses cytochrome *c* release and inhibits apoptosis (Pastorino et al., 2002; Wilson, 2003). To determine whether mitochondrial hexokinases play a direct role in the regulation of plant PCD, we examined whether the exogenous addition of Hxk1 can inhibit stimulus-induced cytochrome *c* release from mitochondria. We first prepared the recombinant full-length Hxk1 (Met-1 to Ser-497) and Hxk1ΔN (Met-28 to Ser-497), which lacks the N-terminal membrane anchor. The *Hxk1* cDNA fragments encoding the full-length Hxk1 and Hxk1ΔN were cloned into the pET21a expression vector and expressed in *Escherichia coli*. The recombinant proteins were affinity-purified using the C-terminal His tag, yielding polypeptides of ~55 and ~52 kD (see Supplemental Figures 3A and 3B online), which are consistent with the predicted sizes of Hxk1 and Hxk1ΔN, respectively.

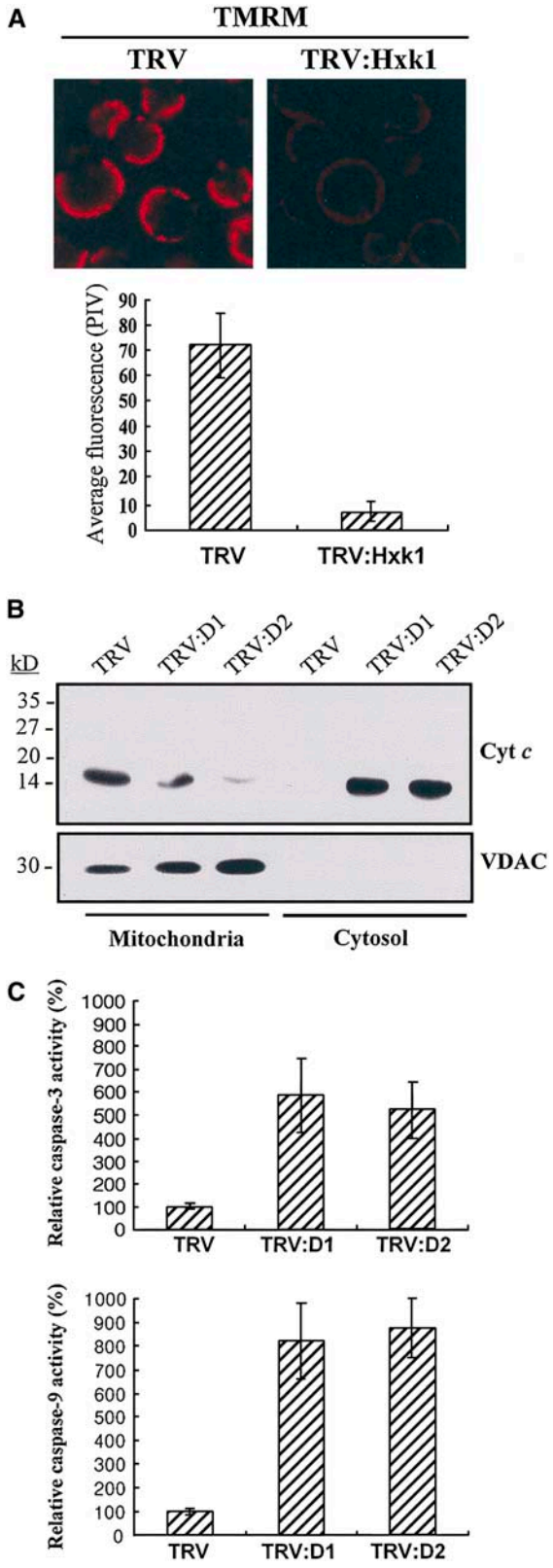


**Figure 6.** Disrupted Mitochondrial Membrane Integrity, Cytochrome *c* Release, and Caspase Activity.

A mitochondria-enriched fraction was prepared from *N. benthamiana* leaves. The mitochondria-enriched fraction was left untreated or was treated with 20 μM CTZ, 10 mM $H_2O_2$, or 20 μM CTZ and 10 mM $H_2O_2$ for 1 h (Figure 8A). CTZ, an antifungal azole derivative, dissociates hexokinases from mitochondria in a dose-dependent manner, in addition to its role as a calmodulin antagonist (Penso and Beitner, 1998; Pastorino et al., 2002; Majewski et al., 2004). The fraction was pelleted to remove mitochondria, and the resulting supernatant was subject to SDS-PAGE. Cytochrome *c* released from the mitochondria into the supernatant was detected by protein gel blot analysis using an anti–cytochrome *c* antibody. The CTZ treatment alone resulted in almost no release of cytochrome *c* from the mitochondria compared with the untreated control sample, whereas $H_2O_2$ treatment for 1 h caused a slight increase in cytochrome *c* release. However, when the two agents were combined, there was a marked increase in cytochrome *c* release from the mitochondria into the supernatant, indicating that CTZ potentiated $H_2O_2$-induced cytochrome *c* release (Figure 8A). Next, recombinant Hxk1 and Hxk1ΔN at concentrations ranging from 1 to 50 μg/mL were incubated for 30 min with the mitochondria-enriched fraction before CTZ and $H_2O_2$ treatment, and the effects of the exogenously applied Hxk1 and Hxk1ΔN on CTZ/$H_2O_2$-induced cytochrome *c* release were examined (Figure 8B). Although Hxk1 at the lower concentrations (up to 2.5 μg/mL) was unable to prevent cytochrome *c* release, Hxk1 at the higher concentrations blocked cytochrome *c* release in a dose-dependent manner. With 50 μg/mL Hxk1, the level of cytochrome *c* in the supernatant was similar to that of the untreated samples, suggesting almost complete reduction in the cytotoxic effect of CTZ/$H_2O_2$. By contrast, Hxk1ΔN at various concentrations was unable to prevent CTZ/$H_2O_2$-induced cytochrome *c* release. These results indicate that the Hxk1 association with mitochondria is critical for the inhibition of cytochrome c release (Figure 8B).

To examine the effects of glucose availability on PCD, the mitochondria-enriched fraction was incubated with glucose (0 to 10 mM) for 30 min before CTZ/$H_2O_2$ treatment (Figure 8C). Exposing the mitochondria to increasing amounts of glucose suppressed the cytochrome *c* release dose-dependently,

**(A)** Mitochondrial membrane integrity. Protoplasts isolated from leaves of TRV or TRV:Hxk1 VIGS lines were stained with 200 nM TMRM for 2 min to visualize mitochondria. The average fluorescence was quantified as described in Methods. Data points represent means ± SD of 14 to 15 individual protoplasts. PIV, pixel intensity value.

**(B)** Immunodetection of cytochrome *c* in mitochondrial and cytosolic fractions of leaves from TRV, TRV:Hxk1(D1), and TRV:Hxk1(D2) VIGS lines. Protein gel blotting with a cytochrome *c* monoclonal antibody shows cytochrome *c* release into the cytosol in the TRV:Hxk1 lines. Protein gel blotting with an anti-VDAC monoclonal antibody was used as a control for cell fractionation. VDAC is localized to the outer mitochondrial membrane (Tsujimoto and Shimizu, 2002).

**(C)** Activation of caspase-9– and caspase-3–like activity. Extracts from leaves of TRV or TRV:Hxk1(D1) and TRV:Hxk1(D2) VIGS lines were incubated with fluorogenic peptide substrates of caspase-9 (LEHD-AFC) and caspase-3 (DEVD-AFC) in caspase assay buffer, and the relative fluorescence was measured. Enzymatic activity was normalized for protein concentration and expressed as a percentage of activity present in control extracts. Data points represent means ± SD of three experiments per line.

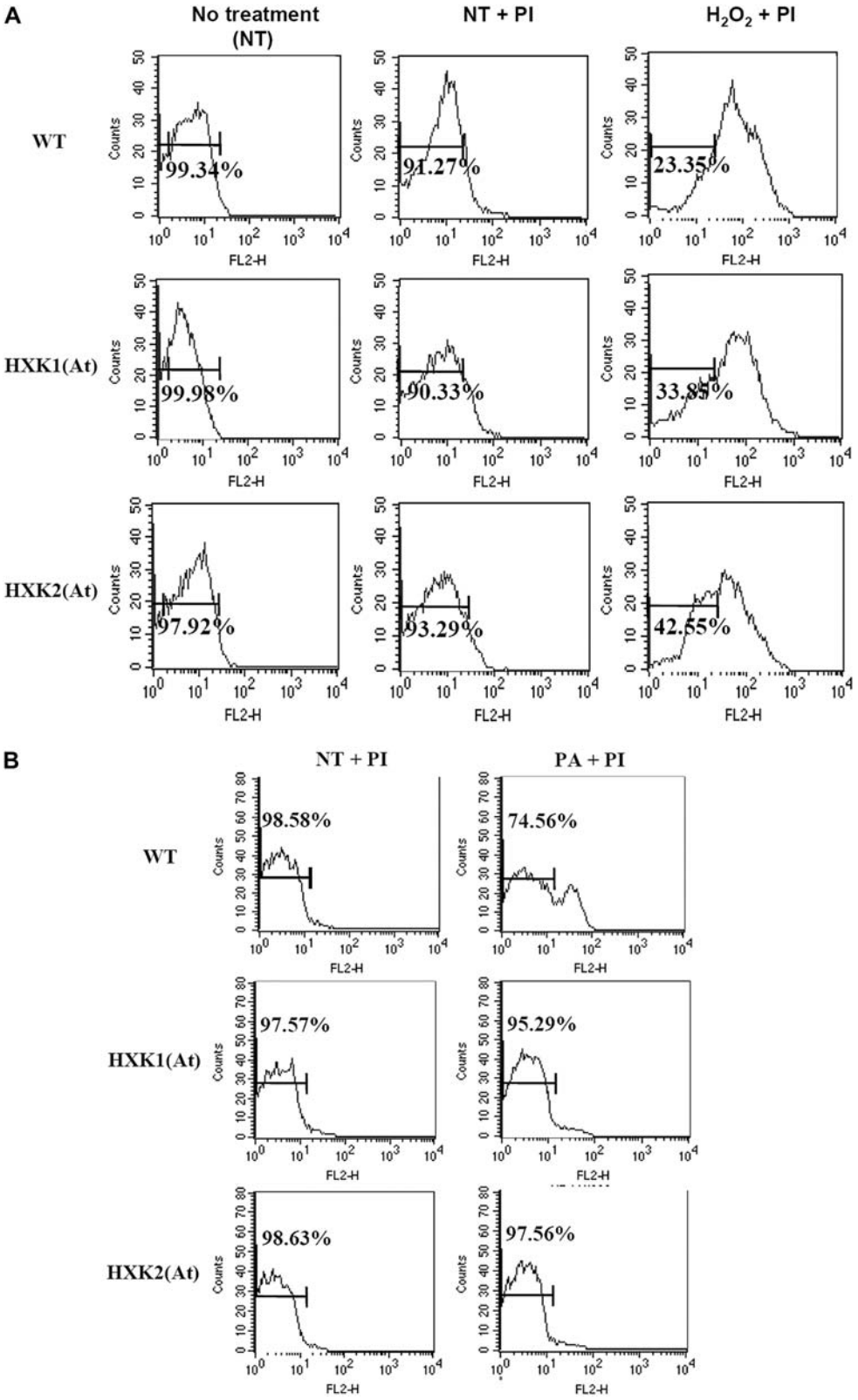


**Figure 7.** Flow Cytometry Analysis of $H_2O_2$- and α-Picolinic Acid–Induced Cell Death.

Protoplasts isolated from wild-type, HXK1-overexpressing, and HXK2-overexpressing *Arabidopsis* plants were treated with 10 mM $H_2O_2$ for 6 h **(A)** or with 0.5 mg/mL α-picolinic acid (PA) for 3 h **(B)** before staining with propidium iodide (PI). Flow cytometry analysis was conducted using 10,000 protoplasts per sample. Data are presented in histograms of propidium iodide fluorescence (FL2) versus cell number. Percentages of live protoplasts are indicated. Data are representative of three independent experiments.

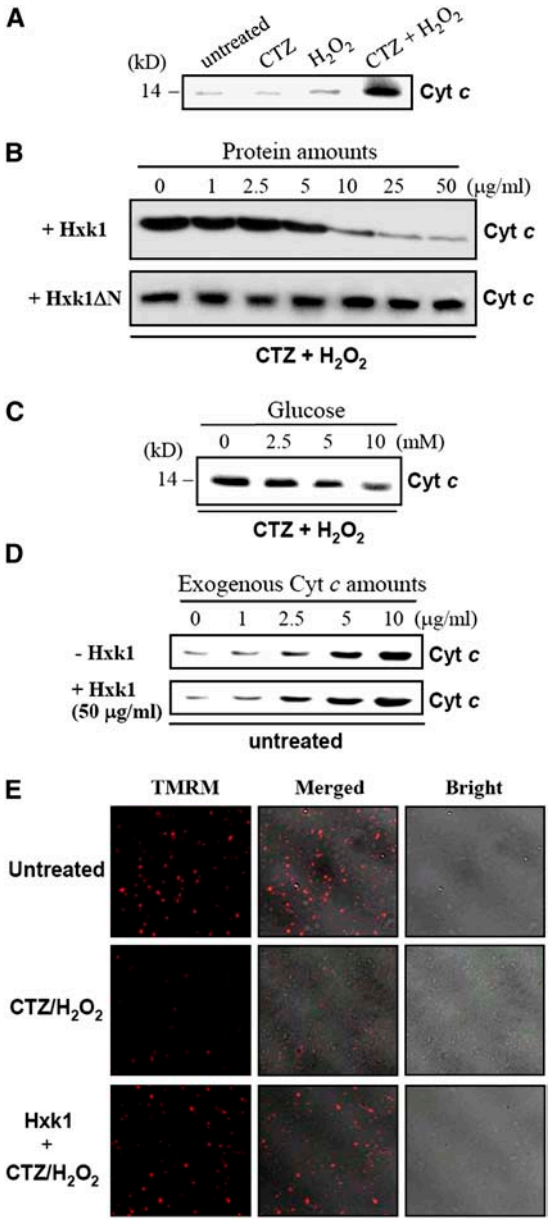


**Figure 8.** Effects of Hxk1 on Cytochrome *c* Release from Isolated Mitochondria.

**(A)** The mitochondria-enriched fraction was prepared from *N. benthamiana* leaves. The mitochondria-enriched fraction was left untreated or treated with 20 μM CTZ, 10 mM $H_2O_2$, or 20 μM CTZ and 10 mM $H_2O_2$ for 1 h at 30°C. The fraction was then centrifuged, and the resulting supernatant was subject to 12% SDS-PAGE. Cytochrome *c* was detected by protein gel blot analysis using an anti–cytochrome *c* antibody.

**(B)** The mitochondria-enriched fraction (50 μL) was incubated with the recombinant Hxk1 and Hxk1ΔN proteins at various concentrations (0, 1, 2.5, 5, 10, 25, and 50 μg/mL) for 30 min at 30°C. Then, the fraction was treated with 20 μM CTZ and 10 mM $H_2O_2$ for 1 h at 30°C. After centrifugation to pellet mitochondria, the resulting supernatant (20 μL) was separated by 12% SDS-PAGE. Cytochrome *c* in the supernatant was detected by protein gel blot analysis using an anti–cytochrome *c* antibody.

**(C)** The mitochondria-enriched fraction was incubated with glucose (0 to 10 mM) for 30 min before CTZ/$H_2O_2$ treatment to examine the effect of glucose availability. The amount of cytochrome *c* in the supernatant was analyzed by protein gel blotting.

**(D)** To exclude the possibility of nonspecific binding between cytochrome *c* and Hxk1, cytochrome *c* (1 to 10 μg/mL) was exogenously added to the mitochondrial fraction that was preincubated with or without Hxk1 (50 μg/mL). After a 1-h incubation, the amount of free cytochrome *c* in the supernatant was analyzed by protein gel blotting.

**(E)** The protective effect of Hxk1 was examined by TMRM staining of mitochondria. TMRM accumulates in mitochondria in proportion to the mitochondrial membrane potential. Before TMRM staining, the mitochondria-enriched fraction was untreated, treated with CTZ/$H_2O_2$, or treated with CTZ/$H_2O_2$ after preincubation with Hxk1 (50 μg/mL).

suggesting the presence of intrinsic glucose-dependent anti-apoptotic mechanisms that presumably involve endogenous hexokinase activity. To exclude the possibility that cytochrome *c* released in response to CTZ/$H_2O_2$ treatment nonspecifically binds to mitochondria-bound Hxk1 and is thereby retained in the mitochondrial pellet, increasing amounts of cytochrome *c* (1 to 10 μg/mL) were added to mitochondrial fractions that were preincubated with or without Hxk1 (50 μg/mL) (Figure 8D). After a 1 h incubation, the supernatant was analyzed for the amount of free cytochrome *c*. Regardless of the amount of cytochrome *c* added, the free cytochrome *c* level remained unaffected by Hxk1 addition, indicating that Hxk1 does not bind to cytochrome *c*. Finally, we visualized the protective effects of Hxk1 by TMRM staining, an indicator of mitochondrial membrane potential (Figure 8E). The mitochondrial fraction was untreated, treated with CTZ/$H_2O_2$, or treated with CTZ/$H_2O_2$ after preincubation with Hxk1 (50 μg/mL). The mitochondrial fractions were then briefly stained with TMRM and observed by confocal laser scanning microscopy. The CTZ/$H_2O_2$ treatment significantly reduced the TMRM fluorescence of the mitochondria, indicating a disruption in the mitochondrial membrane potential. However, the Hxk1 preincubation fully prevented the loss of TMRM fluorescence, indicating a cytoprotective function of Hxk1.

## DISCUSSION

In this study, we present direct evidence that hexokinase is involved in the regulation of PCD in plants. First, interruption of hexokinase function activated PCD in plant cells. When the expression of *Hxk1* encoding a mitochondria-associated hexokinase was suppressed by VIGS, the affected cells showed characteristic features of apoptotic cell death, including nuclear condensation and DNA fragmentation. This hexokinase-mediated cell death pathway involves ROS, cytochrome *c* release from mitochondria, activation of caspase-like activities, and transcriptional induction of cell death–related genes. Second, increased hexokinase activity partially prevented acute oxidant-induced cell death. Overexpression of *Arabidopsis HXK1* and *HXK2*, both of which encode predominantly mitochondria-associated hexokinases, conferred enhanced resistance against $H_2O_2$ and α-picolinic acid. Finally, the recombinant Hxk1 protein prevented CTZ/$H_2O_2$-induced cytochrome *c* release from the mitochondria and the disruption of mitochondrial membrane potential.

Recent findings have suggested that mitochondria-associated hexokinases play a role in the regulation of survival signaling and apoptosis in mammals. Mammalian hexokinase I and II display high-affinity binding to outer mitochondrial membrane contact sites, where they interact with VDAC, and are found in protein complexes containing PT pore constituents (Wilson, 2003). VDAC is a critical component of the mitochondrial PT pore, and the interaction of VDAC with Bcl-2 family proteins, such as proapoptotic BAD and BAX or antiapoptotic BCL-2, controls the release of mitochondrial intermembrane space proteins, which initiate the execution phase of apoptosis (Martinou and Green, 2001). Hexokinase binding to VDAC suppresses the release of the intermembrane space proteins and inhibits apoptosis (Pastorino et al., 2002). Furthermore, the Ser/Thr kinase Akt, which is known to transmit survival signals and to inhibit apoptosis, is required to maintain hexokinase association with mitochondria (Gottlob et al., 2001; Majewski et al., 2004). Thus, targeted disruption of the mitochondria–hexokinase interaction and exposure to proapoptotic stimuli that promote the rapid dissociation of hexokinase from mitochondria strongly induce cytochrome *c* release and apoptosis (Majewski et al., 2004). Conversely, increased hexokinase activity protects animal cells against BAX- or oxidant-induced apoptosis (Bryson et al., 2002; Pastorino et al., 2002). A recent study demonstrated that glucokinase (hexokinase IV) resides in a large functional holoenzyme complex in mitochondria, together with BAD, protein kinase A, protein phosphatase I catalytic subunit, and WAVE-1 as a protein kinase A–anchoring protein (Danial et al., 2003). Glucose promotes the phosphorylation of BAD, and the glucokinase associated with phosphorylated BAD has higher activity than that associated with unphosphorylated BAD. Thus, BAD not only influences glucose metabolism but also responds to abnormalities in glucose metabolism by triggering apoptosis (Danial et al., 2003; Downward, 2003). These results indicate a role for hexokinase and BAD in integrating pathways of glucose metabolism and apoptosis.

Plant hexokinases are found as multiple isoforms and are localized in various subcellular compartments, including the cytosol, mitochondria, chloroplasts, and nucleus. Very little is known about the intracellular localization and biochemical characteristics of each individual hexokinase isoform. In maize (*Zea mays*) roots, 43% of the total hexokinase activity was recovered in the mitochondrial fraction and 35% in the cytosol after tissue homogenization (Galina et al., 1995), indicating that a major part of cellular hexokinase activity comes from the mitochondria-associated hexokinase in maize roots. Furthermore, the mitochondrial and cytosolic hexokinases possess different biochemical characteristics, notably different sensitivity to inhibition by ADP (Galina et al., 1995). Recently, Giegé et al. (2003) used a proteomic analysis to show that the functional glycolytic pathway, including two isoforms of hexokinase (HXK2 and a putative hexokinase), is associated with the outside of the mitochondrion in *Arabidopsis*. The authors proposed that all of the enzymes of the glycolytic pathway interact directly with one another through protein–protein binding to form a glycolytic metabolon on the cytoplasmic face of the outer mitochondrial membrane, allowing pyruvate to be provided directly to the mitochondria as a substrate for respiration to integrate glycolysis and mitochondrial energy metabolism (Giegé et al., 2003; Rolland and Sheen, 2005). HXK1, HXK2, and other hexokinase-like proteins of *Arabidopsis* all appeared to be associated primarily with mitochondria (B. Moore and J. Sheen, unpublished data, cited in Rolland and Sheen, 2005), possibly using the N-terminal membrane anchor domain like Hxk1.

The nature of the hexokinase binding site in plant mitochondria is currently unknown, but it is tempting to speculate that plant hexokinases are also anchored to the mitochondrial membrane through interactions with VDAC. Plant VDAC isoforms yielded voltage-dependent anion channels with electrophysiological parameters comparable to known animal VDACs when reconstituted into planar phospholipid bilayers (Elkeles et al., 1997). Furthermore, VDAC is a conserved element of the PCD pathways in both plant and animal systems (Godbole et al., 2003). Thus, by controlling VDAC and the PT pore in mitochondria, plant hexokinase may regulate cytochrome *c* release into the cytosol and the subsequent execution of cell death. Indeed, this study showed that the exogenous addition of Hxk1 into the mitochondrial fraction, but not the addition of the deletion mutant Hxk1ΔN lacking mitochondrial binding activity, could suppress the early apoptotic effects of CTZ/$H_2O_2$ (Figures 8B and 8E). The effects of CTZ action in plant cells are not known, but in this study, CTZ, combined with $H_2O_2$, produced high cytotoxicity, modifying outer mitochondrial membrane permeability, leading to cytochrome *c* release. These results suggest that Hxk1 association with mitochondria is critical to maintaining outer mitochondrial membrane integrity against the reactivity of $H_2O_2$ and CTZ. Hxk1 association may directly influence the structure and conductance of VDAC to inhibit the opening of the PT pore, similar to hexokinase action in animal systems (Vyssokikh and Brdiczha, 2003). In this scenario, an increase in mitochondria-associated hexokinase activity would have protective benefits for cell survival against apoptotic stimuli. Conversely, the dissociation of mitochondrial hexokinases may reduce the ability of a cell to maintain mitochondrial integrity under stress conditions, which may lead to the activation of PCD. Although the precise mechanism underlying the antiapoptotic effect of hexokinases remains to be determined, this study indicates a critical role of mitochondria-bound hexokinases in the regulation of plant PCD.

In this study, we observed that exogenous glucose partially prevented the CTZ/$H_2O_2$-induced apoptotic response (Figure 8C). Protective effects of glucose against oxidant-induced cell death have been observed in animal systems. The addition of glucose to rat brain mitochondria increased the rate of oxygen consumption and reduced the rate of $H_2O_2$ generation (da-Silva et al., 2004). In addition, the salutary effect of ectopic hexokinase expression during oxidative stress was glucose-dependent in renal epithelial cells (Bryson et al., 2002). The mechanism of the protective effect of exogenous glucose observed in this study is not known, but a glucose-induced conformational change in mitochondrial hexokinase may affect the PT pore configuration and thereby suppress cytochrome *c* release.

We found that the cellular glucose kinase activity in the *Hxk1* VIGS plants was ~31% of that of the TRV controls, whereas the fructose kinase activity was similar to control levels (Figure 3). The *Arabidopsis HXK1* null mutant *gin2*, which retained ~50% of its glucose phosphorylation activity, did not show the cell death

phenotype, although the mutation caused cell expansion defects and delayed senescence (Moore et al., 2003). This may indicate that the hexokinase level must be reduced below a certain threshold level to activate PCD. Although *Hxk1* was targeted for VIGS, the expression of *Hxk1* homologs appeared to be affected as well, because the ~0.4-kb VIGS construct containing the C-terminal end and the 3′ untranslated region sequence of *Hxk1* did not result in the PCD phenotype (data not shown). Previously, a 23-nucleotide DNA fragment bearing 100% identity to a target gene was shown to be the minimum required for gene silencing (Thomas et al., 2001). However, a 23-nucleotide sequence is often not sufficient to initiate silencing, and longer identical sequences must sometimes be used (Thomas et al., 2001). In *Arabidopsis*, *HXK1* and *HXK2* are substantially different in nucleotide sequences from the other four genes encoding hexokinase-like proteins, and a 25-nucleotide perfect sequence match was not found between the two groups of genes (data not shown). Therefore, the cell-death phenotype observed in this study is likely to be caused by gene silencing of only a subset of hexokinases that are homologous with Hxk1, possibly all of them being mitochondria-associated. The enhanced resistance to $H_2O_2$- and α-picolinic acid–induced cell death by the overexpression of *Arabidopsis HXK1* and *HXK2* (Figure 7) also supports the hypothesis that mitochondria-associated hexokinases play a crucial role in mitochondria-dependent PCD in plant cells.

Because cellular homeostasis is critically dependent on energy status, PCD, as a process for maintaining cellular homeostasis, might be dependent on glucose metabolism. In this study, reduced hexokinase activity induced PCD, indicating that PCD and glucose metabolism might be linked via mitochondria-bound hexokinases in plant cells. It will be interesting to investigate whether other glycolytic enzymes are also involved in PCD in plants. For example, in animal studies, glyceraldehyde-3-phosphate dehydrogenase (GAPDH) was shown to have a proapoptotic role in cultured neurons (Ishitani and Chuang, 1996; Saunders et al., 1999; Tajima et al., 1999) in addition to its role as a cell cycle–dependent transcriptional regulator (Zheng et al., 2003). GAPDH isoforms were translocated to the nucleus during neuronal apoptosis (Saunders et al., 1999), and downregulation of GAPDH using antisense oligonucleotides inhibited apoptosis, whereas overexpression promoted apoptosis (Ishitani and Chuang, 1996; Tajima et al., 1999). Hexokinases and a few glycolytic enzymes (lactate dehydrogenase and enolase) are also localized in the nucleus as components of transcriptional coactivators or repressors in yeast and mammals (Kim and Dang, 2005). Interestingly, plant hexokinases are also found in the nuclear fraction, suggesting that hexokinase may control gene expression directly as a universal glucose signaling mechanism in eukaryotic cells (Yanagisawa et al., 2003). Together, these results suggest the intriguing possibility that glycolytic enzymes may have multifaceted roles in both animal and plant cells.

## METHODS

### VIGS

*Nicotiana benthamiana* plants were grown in a growth room at 24°C under a regime of 16 h of light and 8 h of dark. The 0.72-kb N-terminal and 0.76-kb C-terminal fragments and the full length *Hxk1* cDNA were amplified by PCR and cloned into the pTV00 vector containing part of the TRV genome (Ratcliff et al., 2001) using the *Bam*HI and *Apa*I sites. VIGS was performed as described (Ratcliff et al., 2001; Kim et al., 2003; Cho et al., 2004). For RT-PCR and various cytological experiments, the fourth or fifth leaf above the infiltrated leaf was used.

### Subcellular Localization of Hxk1

The *Hxk1* cDNA fragments corresponding to the full-length Hxk1 (Met-1 to Ser-497) and the N-terminal deletion mutant Hxk1ΔN (Met-28 to Ser-497) were cloned into the 326-GFP plasmid using *Bam*HI sites to generate the Hxk1:GFP and Hxk1ΔN:GFP fusion proteins. The two different GFP fusion constructs and the mitochondrial $F_1$ATPase-γ:RFP fusion construct were introduced into *Arabidopsis thaliana* protoplasts prepared from whole seedlings by polyethylene glycol–mediated transformation (Cho et al., 2004). Expression of the fusion constructs was monitored 24 h after transformation by confocal laser scanning microscopy, as described (Cho et al., 2004).

### RT-PCR and RNA Gel Blot Analysis

*N. benthamiana* seeds were surface-sterilized and plated on Murashige and Skoog salts medium (Gibco BRL) solidified with 0.4% Phytagel (Sigma-Aldrich). Seedlings were grown under sterile conditions for 2 weeks. A 10 mM $H_2O_2$ solution was poured directly onto the plates containing 2-week-old seedlings, followed by incubation for the indicated times. For heat treatment, the plates containing 2-week-old seedlings were incubated at 55°C for the indicated times. For thapsigargin treatment, detached young leaves from *N. benthamiana* plants grown for 7 weeks were incubated with water or 100 μM cycloheximide for 2 h, then transferred to 300 μM thapsigargin and incubated for the indicated times. Plant materials were frozen in liquid nitrogen and stored at −70°C for RNA extraction.

Total RNA was prepared with TRIzol reagent (Invitrogen) according to the manufacturer's instructions. RT-PCR was performed with 10 μg of total RNA as described (Kim et al., 2003). To detect the endogenous hexokinase transcripts, the primer sets HXK-A (5′-GGTACAGGGACCAAT-3′ and 5′-CTTCAAGGTACATTG-3′), HXK-B (5′-GAAGAAAGCGACGGTG-3′ and 5′-ACCAAGATCCAACGC-3′), and HXK-C (5′-GACAAGCTGAAGGAT-3′ and 5′-CTTCAAGGTACATTG-3′) were used. To detect the cell death–related transcripts, the previously described primers were used for RT-PCR (Kim et al., 2003). For RNA gel blot analysis, ~30 μg of total RNA was separated by electrophoresis on an agarose gel containing 5.1% (v/v) formaldehyde and blotted onto a Zeta-probe GT genomic-tested blotting membrane (Bio-Rad). Prehybridization and hybridization were performed according to the manufacturer's instructions. The ~0.2-kb DNA fragment containing the 3′ untranslated region of the *Hxk1* cDNA was used as a probe.

### Measurement of Hexokinase Activity and Hexose Phosphate Content

Leaf hexose phosphorylation activities using glucose and fructose as substrates were measured by an enzyme-linked assay, as described previously (Moore et al., 2003). Glucose-6-phosphate and fructose-6-phosphate contents in the leaves of TRV and TRV:Hxk1 lines were also measured by an enzyme-linked assay, as described previously (Moore et al., 2003).

### DNA Fragmentation Analysis

Genomic DNA was isolated from the fourth leaf above the infiltrated leaf in the VIGS lines using a Genome Isolation Kit (Qiagen) according to the

manufacturer's instructions. Genomic DNA (5 μg) was separated on a 1.2% agarose gel and transferred to Hybond $N^+$ membranes (Amersham). As a probe, 100 ng of the total genomic DNA of *N. benthamiana* was labeled with a random labeling kit (Bio-Rad). After hybridization, the membrane was washed with 0.2× SSC (1× SSC is 0.15 M NaCl and 0.015 M sodium citrate) and 0.1% SDS at 60°C for 1 h.

### Histochemical Analyses

Preparation of leaf sections and microscopic observations were performed as described previously (Kim et al., 1998; Ahn et al., 2004).

### Measurement of in Vivo $H_2O_2$ and Mitochondrial Membrane Potential

For in vivo $H_2O_2$ measurements, protoplasts isolated from leaves of the VIGS lines were incubated in 2 μM $H_2$DCFDA (Molecular Probes) for 30, 60, 90, 120, and 150 s. Protoplasts were transferred to wells on microscope slides and observed with a confocal microscope (Carl Zeiss LSM 510) with optical filters (488 nm excitation and 505 nm emission) to visualize green fluorescence of the $H_2O_2$-oxidized probe. Quantitative images were captured and data were analyzed using the LSM 510 image-analysis software (version 2.8). For the measurement of mitochondrial membrane potential, 200 nM TMRM (Molecular Probes) was added to protoplasts isolated from leaves of the VIGS lines or to the isolated mitochondria. After incubation for 1 to 2 min at 25°C, the protoplasts or the mitochondria were transferred to microscope slide wells and observed with a confocal microscope (Carl Zeiss LSM 510) with optical filters (543 nm excitation and 585 nm emission) to visualize the red fluorescent probe. Quantitative images were captured and data were analyzed using the LSM 510 software (version 2.8).

### Measurement of Ion Leakage and Evans Blue Staining

Measurement of ion leakage and Evans blue staining were performed as described previously (Kim et al., 2003).

### Localization of Lignin

Leaf samples were incubated in a phloroglucinol-HCl solution for 2 min at room temperature and pressed gently between a slide and a cover slip for observation.

### Cellular Fractionation and Detection of Cytochrome *c* Release

Leaves (2 g) from the VIGS lines were ground in grinding buffer (0.4 M mannitol, 1 mM EGTA, 20 mM 2-mercaptoethanol, 50 mM Tricine, and 0.1% BSA, pH 7.8) for 1 min at 4°C. Extracts were filtered through Miracloth, and the filtrates were centrifuged at 15,000*g* for 5 min at 4°C. The supernatant was centrifuged at 16,000*g* for 15 min at 4°C. After centrifugation, the cytosolic fraction (supernatant) was collected and the mitochondrial fraction (pellet) was resuspended in grinding buffer. Protein samples (50 μg) were separated by electrophoresis using 12% SDS-PAGE, transferred onto polyvinylidene difluoride membranes, and probed with a monoclonal antibody against cytochrome *c* (1:1000 dilution; Pharmingen) and a monoclonal antibody (31HL) against human VDAC (1:1000 dilution; Calbiochem). Antibody binding was detected using horseradish peroxidase–conjugated secondary antibodies and enhanced chemiluminescence (Amersham Pharmacia Biotech).

### Measurement of Caspase-Like Activity

Caspase-like activity was measured as described previously (Kim et al., 2003).

### Flow Cytometry Analysis of Cell Death

Seeds of *HXK1*- and *HXK2*-overexpressing transgenic *Arabidopsis* plants were obtained from Jyan-Chyun Jang (Ohio State University). *Arabidopsis* protoplasts were treated with 10 mM $H_2O_2$ for 3, 6, 12, and 24 h or with 0.5 mg/mL α-picolinic acid for 3 h, and then the number of dead cells was determined using the fluorescent probe propidium iodide. Protoplasts were incubated with 25 μg/mL propidium iodide in culture medium for 5 to 10 min, and propidium iodide staining was quantified in the FL-2 channel of a FACSCalibur instrument (Becton Dickinson) with the Win MDI version 2.8 program (Scripps Research Institute). Each sample for flow cytometry analysis contained 10,000 protoplasts.

### Purification of the Recombinant Hxk1 and Hxk1ΔN

For Hxk1 (Met-1 to Ser-497), the full-length *Hxk1* coding region was amplified by PCR using the primers 5′-GGAATTCATGAAGAAAGCGACG-3′ and 5′-CCCAAGCTTGGACTTATCTTCAAG-3′ containing the *Eco*RI and *Hin*dIII sites, respectively, and cloned into the pET21a vector (Novagen). For Hxk1ΔN (Met-28 to Ser-497), the corresponding cDNA fragment was amplified by PCR using the primers 5′-GGAATTCATGCGCAAATCTAGTAAATG-3′ and 5′-CCCAAGCTTGGACTTATCTTCAAG-3′ and cloned into the pET21a vector. After DNA sequencing for verification, the plasmids containing the Hxk1:$His_{\times 6}$ and Hxk1ΔN:$His_{\times 6}$ genes were transformed into the *Escherichia coli* BL21 (DE3) strain. The *E. coli* cells were treated with 1 mM isopropyl β-D-thiogalactopyranoside for induction, grown for 3 h, and harvested by centrifugation at 6000*g* for 10 min at 4°C. Purification of the Hxk1:$His_{\times 6}$ and Hxk1ΔN:$His_{\times 6}$ proteins was performed according to the manufacturer's instructions. One liter of cell lysate was loaded onto an IDA-MiniExcellose affinity column (Bioprogen), and the column was washed three times with 10 mL of equilibration buffer (50 mM phosphate and 0.5 N NaCl, pH 8.0). The recombinant protein was eluted with 5 mL of 0.5 M imidazole in the equilibration buffer and dialyzed in dialysis buffer (50 mM Tris-HCl, pH 8.0) for 48 h at 4°C. Hxk1 was concentrated using ultrafiltration (molecular weight cutoff, 10,000; Amicon) to a final concentration of 0.5 mg/mL.

### Effect of Hxk1 on Cytochrome *c* Release from Mitochondria

The mitochondria-enriched fraction was isolated from *N. benthamiana* leaves and suspended in the mitochondrial buffer (0.4 M mannitol, 1 mM EGTA, 20 mM 2-mercaptoethanol, 50 mM Tricine, and 0.1% BSA, pH 7.8). The mitochondria-enriched fraction (50 μL) was left untreated or treated with 20 μM CTZ, 10 mM $H_2O_2$, or 20 μM CTZ and 10 mM $H_2O_2$ for 1 h at 30°C. To observe the effect of added hexokinases, the mitochondria-enriched fraction was incubated with the recombinant Hxk1 and Hxk1ΔN proteins at concentrations ranging from 1 to 50 μg/mL for 30 min at 30°C and then treated with 20 μM CTZ and 10 mM $H_2O_2$ for 1 h at 30°C in the mitochondrial buffer. For the determination of cytochrome *c* release, the mitochondria-enriched fraction was pelleted at 16,000*g* for 15 min at 4°C, and the resulting supernatant (20 μL) was subjected to 12% SDS-PAGE. The released cytochrome *c* in the supernatants was detected by protein gel blot analysis using the monoclonal antibody against cytochrome *c* (1:1000 dilution; Pharmingen). To observe the effects of exogenously added glucose, the mitochondria-enriched fraction was preincubated with glucose at concentrations ranging from 2.5 to 10 mM for 30 min at 30°C before treatment with 20 μM CTZ and 10 mM $H_2O_2$ for 1 h at 30°C. To determine whether Hxk1 binds to cytochrome *c*, varying amounts of cytochrome *c* (1 to 10 μg/mL) were added to the mitochondria-enriched fraction that was preincubated with or without Hxk1 (50 μg/mL) for 30 min at 30°C. After a 1-h incubation at 30°C, the cytochrome *c* amount in the supernatant was analyzed as described above.

### Accession Numbers

The GenBank accession number for Hxk1 of *Nicotiana benthamiana* is AY286011.

### Supplemental Data

The following materials are available in the online version of this article.

**Supplemental Figure 1.** Alignment of Hxk1 and Related Sequences.

**Supplemental Figure 2.** Expression Analysis of *Hxk1*.

**Supplemental Figure 3.** Purification of the Recombinant Hxk1 and Hxk1ΔN.

## ACKNOWLEDGMENTS

The authors thank Jyan-Chyun Jang (Ohio State University) for providing seeds of *HXK1*- and *HXK2*-overexpressing *Arabidopsis* transgenic lines, Jen Sheen (Harvard Medical School) for providing the protocols to measure hexokinase activity and hexose phosphate content, and David C. Baulcombe (John Innes Centre) for providing VIGS vectors. This research was supported by the grants from the Plant Diversity Research Center of the 21st Century Frontier Research Program, the Molecular and Cellular BioDiscovery Program, and the Plant Signaling Network Research Center (at Korea University) of the Science Research Center Program, all of which are funded by the Ministry of Science and Technology of Korea. Funding for M.K. was provided by the Nano/Bio Science and Technology Program.

Received January 30, 2006; revised June 25, 2006; accepted July 18, 2006; published August 18, 2006.

## REFERENCES

**Ahn, J.-W., Kim, M., Lim, J.H., Kim, G.-T., and Pai, H.-S.** (2004). Phytocalpain controls the proliferation and differentiation fates of cells in plant organ development. Plant J. **38,** 969–981.

**Austin, M.J., Muskett, P., Kahn, K., Feys, B.J., Jones, J.D., and Parker, J.E.** (2002). Regulatory role of SGT1 in early R gene-mediated plant defenses. Science **295,** 2077–2080.

**Azevedo, C., Sadanandom, A., Kitagawa, K., Freialdenhoven, A., Shirasu, K., and Schulze-Lefert, P.** (2002). The RAR1 interactor SGT1, an essential component of R gene-triggered disease resistance. Science **295,** 2073–2076.

**Azoulay-Zohar, H., Israelson, A., Abu-Hamad, S., and Shoshan-Barmatz, V.** (2004). In self-defence: Hexokinase promotes voltage-dependent anion channel closure and prevents mitochondria-mediated apoptotic cell death. Biochem. J. **377,** 347–355.

**Baines, C.P., Kaiser, R.A., Purcell, N.H., Blair, N.S., Osinska, H., Hambleton, M.A., Brunskill, E.W., Sayen, M.R., Gottlieb, R.A., Dorn, G.W., Robbins, J., and Molkentin, J.D.** (2005). Loss of cyclophilin D reveals a critical role for mitochondrial permeability transition in cell death. Nature **434,** 658–662.

**Balk, J., Leaver, C.J., and McCabe, P.F.** (1999). Translocation of cytochrome c from the mitochondria to the cytosol occurs during heat-induced programmed cell death in cucumber plants. FEBS Lett. **463,** 151–154.

**Beers, E.P., Woffenden, B.J., and Zhao, C.** (2000). Plant proteolytic enzymes: Possible roles during programmed cell death. Plant Mol. Biol. **44,** 399–415.

**Bethke, P.C., and Jones, R.L.** (2001). Cell death of barley aleurone protoplasts is mediated by reactive oxygen species. Plant J. **25,** 19–29.

**Birnbaum, M.J.** (2004). On the InterAktion between hexokinase and the mitochondrion. Dev. Cell **7,** 781–782.

**Bryson, J.M., Coy, P.E., Gottlob, K., Hay, N., and Robey, R.B.** (2002). Increased hexokinase activity, of either ectopic or endogenous origin, protects renal epithelial cells against acute oxidant-induced cell death. J. Biol. Chem. **277,** 11392–11400.

**Cho, H.S., Lee, S.S., Kim, K.D., Kim, S.J., Hwang, I., Lim, J.S., Park, Y.I., and Pai, H.-S.** (2004). DNA gyrase is involved in chloroplast nucleoid partitioning. Plant Cell **16,** 2665–2682.

**Danial, N.N., Gramm, C.F., Scorrano, L., Zhang, C.-Y., Krauss, S., Ranger, A.M., Datta, S.R., Greenberg, M.E., Licklider, L.J., Lowell, B.B., Gygi, S.P., and Korsmeyer, S.J.** (2003). BAD and glucokinase reside in a mitochondrial complex that integrates glycolysis and apoptosis. Nature **424,** 952–956.

**Danon, A., Rotari, V.I., Gordon, A., Mailhac, N., and Gallois, P.** (2004). Ultraviolet-C overexposure induces programmed cell death in Arabidopsis, which is mediated by caspase-like activities and which can be suppressed by caspase inhibitors, p35 and defender against apoptotic death. J. Biol. Chem. **279,** 779–787.

**da-Silva, W.S., Gomez-Puyou, A., de Gomez-Puyou, M.T., Moreno-Sanchez, R., De Felice, F.G., de Meis, L., Oliveira, M.F., and Galina, A.** (2004). Mitochondrial bound hexokinase activity as a preventive antioxidant defense: Steady-state ADP formation as a regulatory mechanism of membrane potential and reactive oxygen species generation in mitochondria. J. Biol. Chem. **279,** 39846–39855.

**del Pozo, O., and Lam, E.** (1998). Caspases and programmed cell death in the hypersensitive response of plants to pathogens. Curr. Biol. **8,** 1129–1132.

**Desikan, R., Reynolds, A., Hancock, J.T., and Neill, S.J.** (1998). Harpin and hydrogen peroxide both initiate programmed cell death but have differential effects on defense gene expression in *Arabidopsis* suspension cultures. Biochem. J. **330,** 115–120.

**Downward, J.** (2003). Metabolism meets death. Nature **424,** 896–897.

**Elkeles, A., Breiman, A., and Zizi, M.** (1997). Functional differences among wheat voltage-dependent anion channel (VDAC) isoforms expressed in yeast. Indication for the presence of a novel VDAC-modulating protein? J. Biol. Chem. **272,** 6252–6260.

**Frommer, W.B., Schultze, W.X., and Lalonde, S.** (2003). Hexokinase, jack-of-all-trades. Science **300,** 261–263.

**Galina, A., Reis, M., Albuquerque, M.C., Puyou, A.G., Puyou, M.T., and de Meis, L.** (1995). Different properties of the mitochondrial and cytosolic hexokinases in maize roots. Biochem. J. **309,** 105–112.

**Giegé, P., Heazlewood, J.L., Roessner-Tunali, U., Millar, A.H., Fernie, A.R., Leaver, C.J., and Sweetlove, L.J.** (2003). Enzymes of glycolysis are functionally associated with the mitochondrion in *Arabidopsis* cells. Plant Cell **15,** 2140–2151.

**Giese, J.O., Herbers, K., Hoffmann, M., Klosgen, R.B., and Sonnewald, U.** (2005). Isolation and functional characterization of a novel plastidic hexokinase from *Nicotiana tabacum.* FEBS Lett. **579,** 827–831.

**Godbole, A., Varghese, J., Sarin, A., and Mathew, M.K.** (2003). VDAC is a conserved element of death pathways in plant and animal systems. Biochim. Biophys. Acta **1642,** 87–96.

**Gottlob, K., Majewski, N., Kennedy, S., Kandel, E., Robey, R.B., and Hay, N.** (2001). Inhibition of early apoptotic events by Akt/PKB is dependent on the first committed step of glycolysis and mitochondrial hexokinase. Genes Dev. **15,** 1406–1418.

**Green, D.R., and Kroemer, G.** (2004). The pathophysiology of mitochondrial cell death. Science **305,** 627–629.

**Heath, M.C.** (2000). Hypersensitive response-related death. Plant Mol. Biol. **44,** 321–324.

**Houot, V., Etienne, P., Petitot, A.S., Barbier, S., Blein, J.P., and Suty, L.** (2001). Hydrogen peroxide induces programmed cell death

features in cultured tobacco BY-2 cells in a dose-dependent manner. J. Exp. Bot. **52,** 1721–1730.

**Ishitani, R., and Chuang, D.M.** (1996). Glyceralaldehyde-3-phosphate dehydrogenase antisense oligonucleotides protect against cytosine arabinonucleoside-induced apoptosis in cultured cerebellar neurons. Proc. Natl. Acad. Sci. USA **93,** 9937–9941.

**Jang, J.-C., Leon, P., Zhou, L., and Sheen, J.** (1997). Hexokinases as a sugar sensor in higher plants. Plant Cell **9,** 5–19.

**Kim, G.T., Tsukaya, H., and Uchimiya, H.** (1998). The *ROTUNDIFOLIA3* gene of *Arabidopsis thaliana* encodes a new member of the cytochrome P-450 family that is required for the regulated polar elongation of leaf cells. Genes Dev. **12,** 2381–2391.

**Kim, J.-W., and Dang, C.V.** (2005). Multifaceted roles of glycolytic enzymes. Trends Biochem. Sci. **30,** 142–150.

**Kim, M., Ahn, J.-W., Jin, U.-H., Paek, K.-H., and Pai, H.-S.** (2003). Activation of the programmed cell death pathway by inhibition of proteasome function in plants. J. Biol. Chem. **278,** 19406–19415.

**Leon, P., and Sheen, J.** (2003). Sugar and hormone connections. Trends Plant Sci. **8,** 110–116.

**Lilliehook, C., Chan, S., Choi, E.K., Zaidi, N.F., Wasco, W., Mattson, M.P., and Duxbaum, J.D.** (2002). Calsenilin enhances apoptosis by altering endoplasmic reticulum calcium signaling. Mol. Cell. Neurosci. **19,** 552–559.

**Machida, K., Ohta, Y., and Osada, H.** (2006). Suppression of apoptosis by cyclophilin D via stabilization of hexokinase II mitochondrial binding in cancer cells. J. Biol. Chem. **281,** 14314–14320.

**Majewski, N., Noqueira, V., Bhaskar, P., Coy, P.E., Skeen, J.E., Gottlob, K., Chandel, N.S., Thompson, C.B., Robey, R.B., and Hay, N.** (2004). Hexokinase-mitochondria interaction mediated by Akt is required to inhibit apoptosis in the presence or absence of Bax and Bak. Mol. Cell **16,** 819–830.

**Martinou, J.C., and Green, D.R.** (2001). Breaking the mitochondrial barrier. Nat. Rev. Mol. Cell Biol. **2,** 63–67.

**Mlejnek, P., and Prochazka, S.** (2002). Activation of caspase-like proteases and induction of apoptosis by isopentenyladenosine in tobacco BY-2 cells. Planta **215,** 158–166.

**Moore, B., Zhou, L., Rolland, F., Hall, Q., Cheng, W.-H., Liu, Y.-X., Hwang, I., Jones, T., and Sheen, J.** (2003). Role of the *Arabidopsis* glucose sensor HXK1 in nutrient, light, and hormone signaling. Science **300,** 332–336.

**Nakagawa, T., Shimizu, S., Watanabe, T., Yamaguchi, O., Otsu, K., Yamagata, H., Inohara, H., Kubo, T., and Tsujimoto, Y.** (2005). Cyclophilin D-dependent mitochondrial permeability transition regulates some necrotic but not apoptotic cell death. Nature **434,** 652–658.

**Nimchuk, Z., Eulgem, T., Holt, B.F., III, and Dangl, J.L.** (2003). Recognition and response in the plant immune system. Annu. Rev. Genet. **37,** 579–609.

**Ordenes, V.R., Reyes, F.C., Wolff, D., and Orellana, A.** (2002). A thapsigargin-sensitive $Ca^{2+}$ pump is present in the pea Golgi apparatus membrane. Plant Physiol. **129,** 1820–1828.

**Pastorino, J.G., Shulga, N., and Hoek, J.B.** (2002). Mitochondrial binding of hexokinase II inhibits Bax-induced cytochrome *c* release and apoptosis. J. Biol. Chem. **277,** 7610–7618.

**Penso, J., and Beitner, R.** (1998). Clotrimazole and bifonazole detach hexokinase from mitochondria of melanoma cells. Eur. J. Pharmacol. **342,** 113–117.

**Ratcliff, F., Martin-Hernandez, A.M., and Baulcombe, D.C.** (2001). Tobacco rattle virus as a vector for analysis of gene function by silencing. Plant J. **25,** 237–245.

**Rolland, F., and Sheen, J.** (2005). Sugar sensing and signaling networks in plants. Biochem. Soc. Trans. **33,** 269–271.

**Rolland, F., Winderickx, J., and Thevelein, J.M.** (2001). Glucose-sensing mechanisms in eukaryotic cells. Trends Biochem. Sci. **26,** 310–317.

**Saunders, P.A., Chen, R.W., and Chuang, D.M.** (1999). Nuclear translocation of glyceralaldehyde-3-phosphate dehydrogenase isoforms during neuronal apoptosis. J. Neurochem. **72,** 925–932.

**Stulke, J., and Hillen, W.** (1999). Carbon catabolite repression in bacteria. Curr. Opin. Microbiol. **2,** 195–201.

**Sun, Y.L., Zhao, Y., Hong, X., and Zhai, Z.H.** (1999). Cytochrome c release and caspase activation during menadione-induced apoptosis in plants. FEBS Lett. **462,** 317–321.

**Tajima, H., Tsuchiya, K., Yamada, M., Kondo, K., Katsube, N., and Ishitani, R.** (1999). Over-expression of GAPDH induces apoptosis in COS-7 cells transfected with cloned GAPDH cDNAs. Neuroreport **10,** 2029–2033.

**Thomas, C.L., Jones, L., Baulcombe, D.C., and Maule, A.J.** (2001). Size constraints for targeting post-transcriptional gene silencing and for RNA-directed methylation in *Nicotiana benthamiana* using a potato virus X vector. Plant J. **25,** 417–425.

**Thomas, S.G., and Franklin-Tong, V.E.** (2004). Self-incompatibility triggers programmed cell death in Papaver pollen. Nature **429,** 305–309.

**Travis, A.J., Sui, D., Riedel, K.D., Hofmann, N.R., Moss, S.B., Wilson, J.E., and Kopf, G.S.** (1999). A novel NH(2)-terminal, nonhydrophobic motif targets a male germ cell-specific hexokinase to the endoplasmic reticulum and plasma membrane. J. Biol. Chem. **274,** 34467–34475.

**Tsujimoto, Y., and Shimizu, S.** (2002). The voltage-dependent anion channel: An essential player in apoptosis. Biochimie **84,** 187–193.

**Vyssokikh, M.Y., and Brdiczha, D.** (2003). The function of complexes between the outer mitochondrial membrane pore (VDAC) and the adenine nucleotide translocase in regulation of energy metabolism and apoptosis. Acta Biochim. Pol. **50,** 389–404.

**Wiese, A., Gröner, F., Sonnewald, U., Deppner, H., Lerchl, J., Hebberker, U., Flügge, U.-I., and Weber, A.** (1999). Spinach hexokinase I is located in the outer envelope membrane of plastids. FEBS Lett. **461,** 13–18.

**Wilson, J.E.** (2003). Isozymes of mammalian hexokinase: Structure, subcellular localization and metabolic function. J. Exp. Biol. **206,** 2049–2057.

**Xiao, W., Sheen, J., and Jang, J.-C.** (2000). The role of hexokinase in plant sugar signal transduction and growth and development. Plant Mol. Biol. **44,** 451–461.

**Yanagisawa, S., Yoo, S.-D., and Sheen, J.** (2003). Differential regulation of EIN3 stability by glucose and ethylene signalling in plants. Nature **425,** 521–525.

**Zhang, H., Huang, H.M., Carson, R.C., Mahmood, J., Thomas, H.M., and Gibson, G.E.** (2001). Assessment of membrane potentials of mitochondrial populations in living cells. Anal. Biochem. **298,** 170–180.

**Zhang, H.K., Zhang, X., Mao, B.Z., Li, Q., and He, Z.H.** (2004). Alpha-picolinic acid, a fungal toxin and mammal apoptosis-inducing agent, elicits hypersensitive-like response and enhances disease resistance in rice. Cell Res. **14,** 27–33.

**Zheng, L., Roeder, R.G., and Luo, Y.** (2003). S phase activation of the histone H2B promoter by OCA-S, a coactivator complex that contains GAPDH as a key component. Cell **114,** 255–266.